Journal of Achievements in Materials and Manufacturing Engineering
VOLUME 55
ISSUE 2
December
2012

Friction Stir Lap Welding: material flow, joint structure and strength

Z.W. Chen*, S. Yazdanian
Department of Mechanical Engineering, School of Engineering,
AUT University, Auckland, New Zealand
* Corresponding e-mail address: zhan.chen@aut.ac.nz

Received 19.10.2012; published in revised form 01.12.2012

Manufacturing and processing

ABSTRACT

Friction stir welding has been studied intensively in recent years due to its importance in industrial applications. The majority of these studies have been based on butt joint configuration and friction stir lap welding (FSLW) has received considerably less attention. Joining with lap joint configuration is also widely used in automotive and aerospace industries and thus FSLW has increasingly been the focus of FS research effort recently. number of thermomechancal and metallurgical aspects of FSLW have been studied in our laboratory. In this paper, features of hooking formed during FSLW of Al-to-Al and Mg-to-Mg will first be quantified. Not only the size measured in the vertical direction but hook continuity and hooking direction have been found highly FS condition dependent. These features will be explained taking into account the effects of the two material flows which are speed dependent and alloy deformation behaviour dependent. Strength values of the welds will be presented and how strength is affected by hook features and by alloy dependent local deformation behaviours will be explained. In the last part of the paper, experimental results of FSLW of Al-to-steel will be presented to briefly explain how joint interface microstructures affect the fracturing process during mechanical testing and thus the strength. From the results, tool positioning as a mean for achieving maximum weld strength can be suggested.

Keywords: Hooking; Deformation; Interface intermetallic; Stress concentration; Strength

Reference to this paper should be given in the following way:
Z.W. Chen, S. Yazdanian, Friction Stir Lap Welding: material flow, joint structure and strength, Journal of Achievements in Materials and Manufacturing Engineering 55/2 (2012) 629-637.

1. Introduction

Friction stir welding (FSW) is a solid state joining process and melting/solidification related defects of fusion welding are avoided. Thus, since it was invented in early 1990s [1], FSW has been applied quite widely [2]. Many aspects of FSW have been studied extensively and comprehensively reviewed [3-9]. The majority of FSW studies have been based on butt joint geometry. Lap joint configuration is also widely used in conventional welding and friction stir lap welding (FSLW) should potentially be applied widely, particularly in automotive and aerospace industries. Fig. 1a illustrates FSLW during which a section of lapping surfaces of the top and bottom plates is stirred and mixed in the stir zone (SZ) thus forming a weld behind the tool.

During FSLW of Al-to-Al, Mg-to-Mg or steel-to-steel, material flow affects the un-welded original lapping interface (referred to as un-welded lap hereafter) on both the retreating site and the advancing side. As illustrated in Fig. 1b, upward flow on advancing site of SZ behind the tool drives the material upward and thus a portion of the un-welded lap curves (hooks) up, forming a hook. The hook can be viewed as crack that may orientate favourably for crack growth under loading in service.

In the studies of hooking and its effect on joint properties, a hook size (h) refers to the vertical distance of the hook [10-16] and there has been little attention paid to the actual shape and the

quality (continuity) of the hook. The use of a higher tool rotational speed (ω) or a lower welding speed (v) has been shown to result in a larger *h* [14-16], although the detailed thermomechanical reasons have not been more accurately explained. It is generally understood [10-16] that a high h value can result in a lower strength of the lap weld. However, without sufficiently detailed quantification of hooking, a better estimation on how hooking affect weld strength cannot be made. A better understanding on hooking and how it affects weld strength should be critically important for FSLW to be used in automobile and aerospace manufacturing industries.

a)

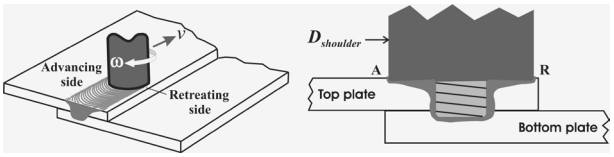

b)

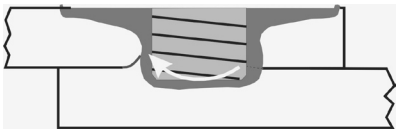

c)

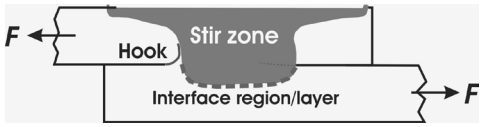

Fig. 1. Schematics illustrations of (a) FSLW and (b) material flow up-lifting un-welded lap thus hooking during FSLW and (c) forces applied to a welded joint during subsequent mechanical testing

Recently, we [17] have conducted a study illustrating that, not only h, but the shape and the continuity of a hook can also influence the fracture strength significantly. FS heat results in softening in various regions of the weld zone. In our recent study [17], the relative roles of hooking and strength property distribution (affected by the thermal cycle during FSLW) affecting the weld strength have been explained for Al-to-Al welds. Furthermore, that referred study has also explained that stress distribution during the commonly used tensile-shear test of FSL welds is highly non-uniform.

Lap welding of dissimilar alloys such as Al-to-steel, Al-to-Ti or Al-to-Cu is also of enormous significance in many industries. In this paper, we focus on an example of FSLW of one metallic alloy to another with considerably higher melting temperature - FSLW of Al-to-steel. In general, it is well known that fusion welding of Al-to-steel is very challenging [18,19]. In FS welding of Al-to-steel, aided by frictional and deformation heat, metallurgical bond is established through diffusion and subsequent formation of interfacial intermetallic, as indicated in Fig. 1c for FSLW. It is clear that a metallurgical bond is a condition for a quality joint, although intermetallics are commonly viewed to affect joint strength adversely [20-22]. How the presence of interface intermetallics affect the joint strength is at present quite unclear in literature.

In the present work, FSLW experiments on Al-to-Al and analysis on how hooking and hook quality affect weld strength will be further conducted. This will be followed by characterising Mg-to-Mg FSL welds and comparing to Al-to-Al welds to illustrate the different hook forming behaviours during FSLW and also the mechanical behaviours during tensile-shear testing due to the difference in local deformation behaviour. In the final section, the work is extended to FSLW of Al-to-steel to explain how interface microstructures affect the fracturing process during tensile-shear testing and thus joint strength. A possible control method for producing Al-to-steel welds for a higher joint strength can then be suggested.

2. Experimental procedures

All FSLW experiments were conducted using a milling machine and thus the mode of FS was displacement control. Schematic illustration of FSLW process has already been provided in Fig. 1. Fig. 2 shows an actual FSLW experiment. A Lowstir™ device, which is also shown in Fig. 2, was used in each FSLW experiment to monitor the downforce (F_z). This monitoring was necessary when a very precise positioning was needed for the case of Al-to-steel welding. Monitoring of temperature in the joining location was also conducted, by placing 0.2 mm K-type thermocouple wires in the lapping location to be FSL welded.

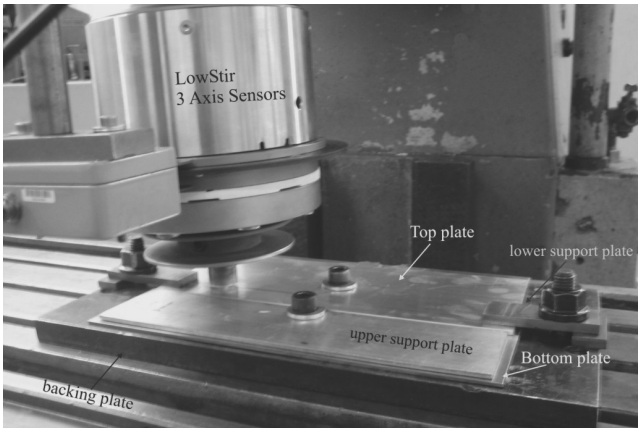

Fig. 2. FSLW using a milling machine with a Lowstir™ force measuring device

Workpiece materials were A6060-T5 aluminium alloy plates (3 mm for Al-to-Al and 6 mm for Al-to-steel), 2.5 mm AZ31B-H24 magnesium alloy and 2 mm mild steel. Both top and bottom plates were 200 mm long and 100 mm wide. Tools were made using H13 tool steel and the left-hand threads of the pins were made with a 1 mm pitch and a 0.6 mm actual depth. The diameter of the concave shoulder was 18 mm for Al-to-Al and Mg-to-Mg FSLW and 20 mm for Al-to-steel FSLW and the pin outside diameter was 6 mm. A tool tilt angle (θ) of 2.5° was used. In the present experiments, v ranged from 20 to 630 mm/min and ω ranged from 500 to 2000 rpm. For the work reported here, the penetration depth

(D_p in Fig. 3) was ~ 1 mm for FSLW of Al-to-Al and Mg-to-Mg and this D_p value varied for FSLW of Al-to-steel.

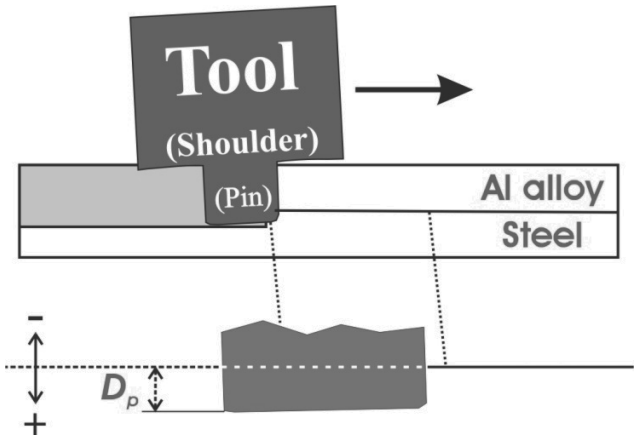

Fig. 3. Schematic illustration of tool positioning during FSLW showing pin penetration depth

Tensile-shear testing of lap welds has been the major method used for evaluating strength of FSL welds in literature. This test method was adopted in this study. Test samples, 16 mm wide, perpendicular to the welding direction were machined from the welded plates. Fig. 4 illustrates the positioning of a sample together with supporting pieces. Samples were tested at a constant crosshead displacement rate of 3 mm/min using a 50 KN Tinus Olsen tensile machine, with a 50 mm extensometer attached. The strength of a lap sample cannot be expressed using the normal load/area, as the stress distribution along the joint area during tensile-shear test is highly uneven. Instead, maximum failure load in a test divided by the width of the sample, F_m/w_s, is taken as strength.

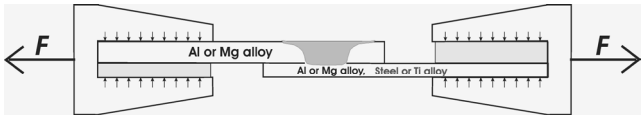

Fig. 4. Schematic illustration of tensile-shear testing

To understand the stress state during tensile-shear testing and how it relates to the location of deformation and fracture, modelling was conducted using Abaqus™ (a FEM model) for predicting the distribution of local stresses in a FSLW joint subjected to axial static load. To obtain an accurate stress value at the crack tip area, very fine meshing has been used. This meshing contains 25,000 elements. Stress distributions were simulated using linear elastic material behaviour.

For microstructure observation, the welds were cross-sectioned, mounted and polished following the normal metallographic procedure. Microstructure examination was conducted using a normal optical microscope and a Hitachi SU-70 FE SEM with a Thermo Scientific NSS EDS/EBSD system.

3. Results and discussion

3.1. Al-to-Al alloy joint structure and strength

Fig. 5 illustrates the general features of hooking and in the figure SZ has been outlined and the hook outside, but very close to, SZ is shown. Material flow in the lower part of SZ during FS with the direction as indicated in the figure pushed up a small portion of the un-welded lap, thus forming the hook. These features are in common with those already described in literature [13-15]. It should be noted that the bell shape of the SZ is primarily the consequence of the combination of the pin related bottom-mid flow and the shoulder related mid-upper flow.

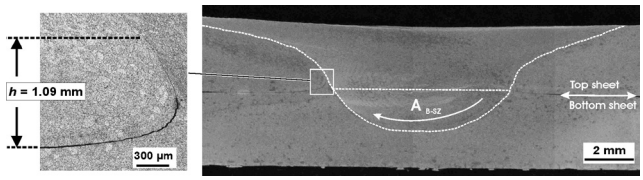

Fig. 5. Cross sectional view of an A6060 weld made using ω = 1,000 rpm and v = 224 mm/min displaying a hook and indicating FS flow direction

In Fig. 6, microfeatures of the hook are further shown. The shape (elongated) and orientation (more dominantly red with orientation shown by the inverse pole figure) of grains in the area including the edge of SZ and thermomechanical affected zone (TMAZ) are clearly different from those in heat affected zone (HAZ) which are largely equiaxed with a different texture (green/blue). It can thus be suggested that not only there is an upward flow induced by the pin during FS, there is a sideward flow (deformation) in the mid-upper region caused by the tool shoulder and the grains were deformed and elongated.

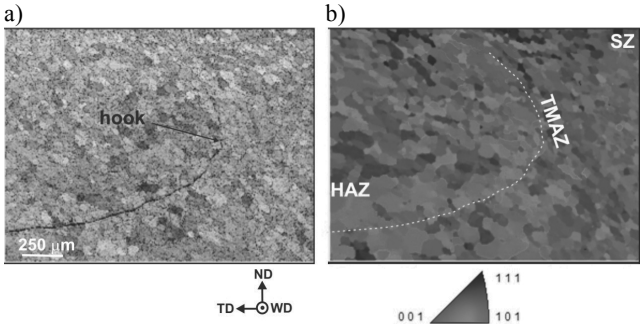

Fig. 6. Hook region in an A6060 weld made using ω = 1,000 rpm and v = 224 mm/min shown by (a) optical micrograph and (b) EBSD orientation map

The upward flow that first causes a hook to form and then the sideward flow shapes the hook to its final orientation, respectively, can thus be suggested and summarised in Fig. 7. The pin related bottom flow first lifts the un-welded lap primarily in TMAZ upward which is the flow direction in TMAZ. Later, the in

the mid-upper region of SZ/TMAZ, the rotating shoulder forges the material not only flowing forward but also sideward due to the material in the upper region being sheared from the retreating side to the advancing side. The upper portion of a hook is thus also forged and sheared sideward and away (from the pin). The size and orientation of a hook thus depend on the intensities of these two flows.

Three traces of hooks in welds made with the same v (112 mm/min) and different ω are shown in Fig. 8. The measured values of bottom SZ areas (referred to as A_{sz} in Fig. 5) are also given. When ω increased from 500 rpm to 1,000 rpm, the increase in A_{sz} clearly increased h, while the sideward flow was strong for both case, resulting in the hooks curving and pointing away. The further increase from 1,000 rpm to 2,000 rpm increased further A_{sz}, but h has remained the same. It should be noted that if any of the hooks was folded back to the original lapping interface location, the end of the hook would not reach the tool pin. This means a part of the original lapping interface has disappeared.

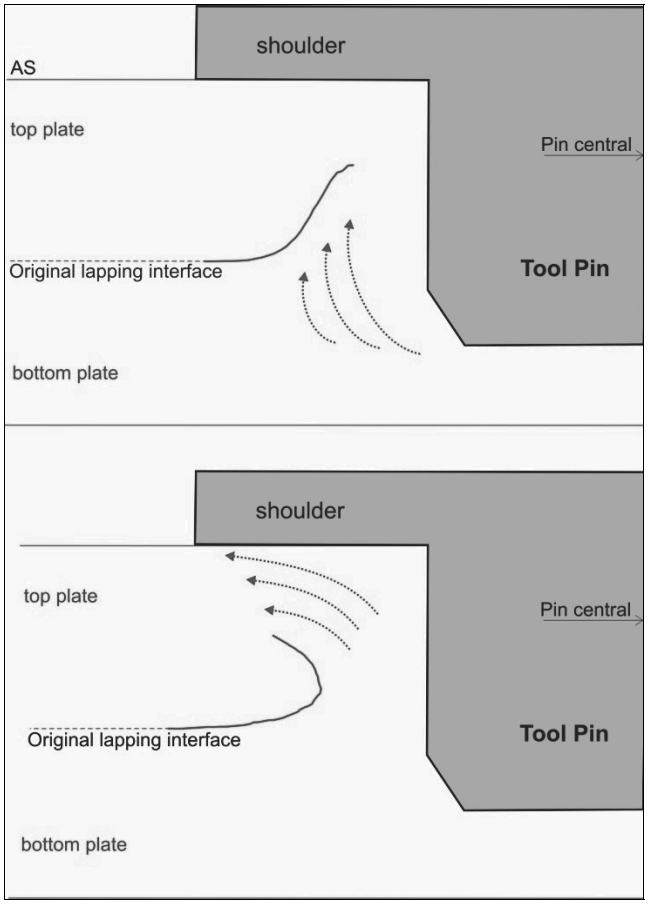

Fig. 7. Schematic illustration of pin and shoulder related upward flow (top) and sideward flow (bottom), respectively

The reason for missing a portion of the original lapping interface becomes clear when features of hooks are examined more closely. Images of two hooks are given in Fig. 9. The two measured h values are almost equal, but the two hooks are very different in both the shape and "quality". On shape, hook A curves significantly more away from the vertical direction than hook B, as expressed by the γ values to be 70° and 46°, respectively. This would mean a stronger sideward flow (more deformation sideward) for hook A. A large amount of deformation (strain) has resulted in the lapping interface becoming more discontinuous and locally closed. Discontinuity is more frequent towards the end. Thus it can be expected that a strong sideward flow should result in part of the section towards the end having closed completely. This is the reason why part of the original lapping interface has disappeared.

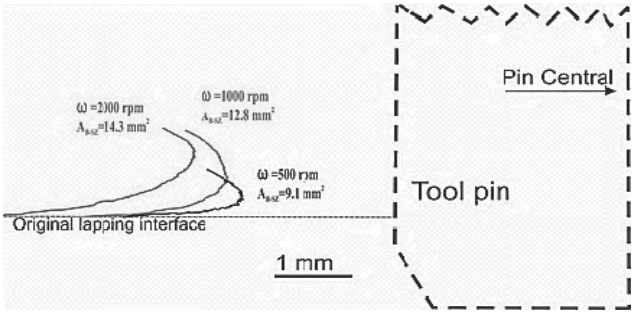

Fig. 8. Hook profiles of A6060 welds made with v = 112 mm/min and ω values shown

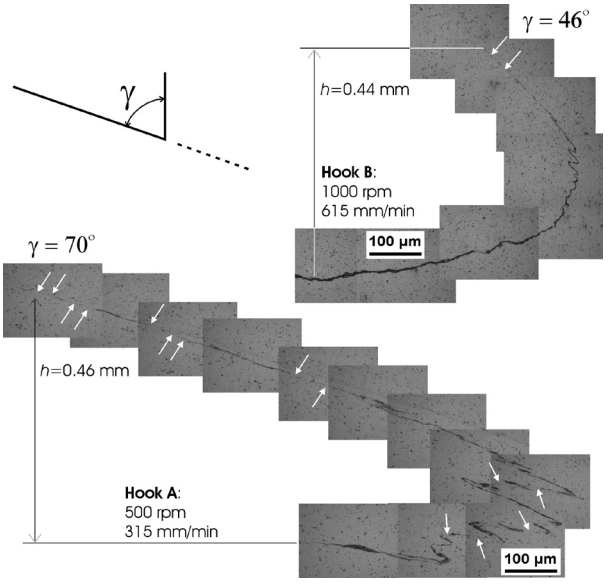

Fig. 9. Micrographs of two hooks of A6060 welds with different hook angles (γ) and local hook discontinuities as pointed to by arrows

Strength (F_m/w_s) values plotted as a function of h are given in Fig. 10. As a comparison, the range of F_m/w_s values of FS bead-on-plate samples using the same alloy plate is provided. A higher ω value or a lower v value normally results in lower F_m/w_s for these bead-on-plate samples. For these samples fracture

locations were all in HAZ, which was also the fracture location for low h samples of FSL welds. For samples with high h values, samples failed by crack propagation from the hook. Data in Fig. 10 have suggested that there is a transition point (h_t) at ~ 0.9 mm. Below h_t, F_m/w_s decreases only slightly as h increases and above h_t, F_m/w_s decreases sharply as h further increases.

A closer examination of the strength values for the samples with $h \approx 0.45$ mm may reveal that not only the size but the shape (suggestive by γ) and the continuity of the hook affect the strength significantly. As discussed and shown in Fig. 9, for hook B (FS with $\omega = 1{,}000$ rpm and $v = 630$ mm/min), hook continuity is high meaning that the hook can largely be treated as a continued crack and γ is lower meaning that the hook orientation is more favourable for the crack to propagate under a tensile-shear load. The crack did propagate from the hook, as predicted. The strength value, at ~ 375 N/mm, is 10-15% lower than the strength values of bead-on-plate samples, corresponding to h/b (b being the thickness of the top plate) = 0.44/3 = 15%. These similar (%) values suggest a thinning effect dominant. The effect of stress concentration is then not apparent.

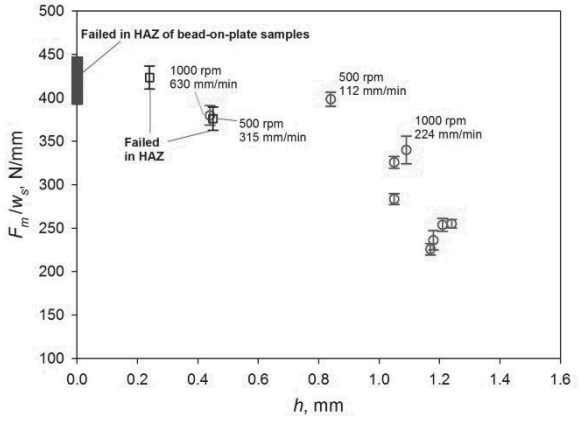

Fig. 10. Strength values plotted as a function of hook size for A6060 welds. Some samples failed in HAZ as indicated and marked blue and other samples (red) cracked from hook

For hook A (Fig. 9) the hook size is very close to that of hook B and strength values for both welds are almost equal, suggesting a size (h) and thus thinning effect dominant. However, for hook A, fracture was in HAZ suggesting that thinning effect on strength is not dominant. As already explained and shown in Fig. 9, for hook A, both hook discontinuity and γ are high. Under loading, deformation and then fracture were in lower strength location, HAZ, and thus the hook and thinning did not affect directly the strength in this case. Although $h = 0.46$ mm, the effective hook size can be treated significantly smaller due to a high degree of discontinuity and a high γ value.

The thinning effect is also not dominant for the samples of weld made using $\omega = 500$ rpm and $v = 112$ mm/min. While h is high at 0.86 mm and $h/b = 0.86/3 = 24.3\%$, $F_m/w_s = 400$ N/mm which is very comparable to the values of bead-on-plate samples. This is because locally hook region can be a region of a significantly higher strength location in comparison to HAZ. It is clear in Fig. 10 that for $h > \sim 0.9$ mm ($h/b = 30\%$) the hook has become too large in size and a slight increase in h caused a sharp decrease in strength.

We now return to the observation that F_m/w_s is not affected by the large stress concentration present in the region around the end of the hook. Stress concentration for tensile-shear testing using a lap joint geometry with $h = 0$ is illustrated in Fig. 11. The applied load is 50 MPa and the highest stress value has reached 170 MPa which is sufficiently high for annealed A6060 to plastically deform. Then the local deformation should result in local bending thus straightening the top and bottom pieces to align more in the loading direction. This new alignment should then reduce considerably or eliminate the stress concentration.

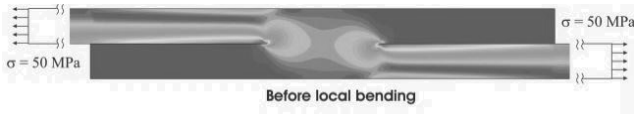

Fig. 11. Simulation result showing distribution of effective stress in the lap location during tensile-shear testing. Red ~ 170 MPa and dark blue 0 MPa

Two tested samples shown in Fig. 12 illustrate the local bending and sample strengthening. When stress concentration is reduced to a very low level, deformation and fracture of the sample will then be away from the region of the hook if thinning effect is not strong. In the case of deformation and fracturing in HAZ of a lap sample, such as the top sample in Fig. 12, the strength should not be significantly different from that of a bead-on-plate sample. Thus there is no reason for a significant reduction in weld strength. This is why strength value of the weld with $h = 0.24$ mm is well within the range of strength values of bead-on-plate samples. Thus, as $h \rightarrow 0$ or even for h/b as high as 8% as shown in Fig. 10, F_m/w_s (lap) $\approx$ F_m/w_s (bead-on-plate). It should be noted that F_m/w_s (bead-on-plate) $\geq$ F_m/w_s (butt).

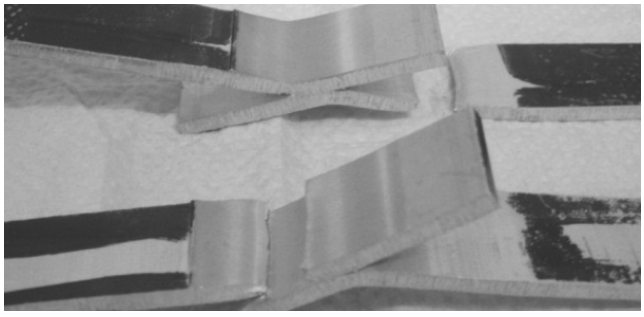

Fig. 12. Tensile-shear tested samples of A6060 welds showing fracture in HAZ (top) and in hook region (bottom), after strengthening

The extensive local plastic deformation before fracturing can be illustrated by a sample shown in Fig. 13. The recrystallized grains in SZ is equiaxed (lower right in Fig. 13) and the grains are extensively elongated due to local deformation before fracturing (lower left in Fig. 13). This highly ductile behaviour during testing (and also during FS) is because there are a high number

of slip systems in Al, as is well known. Then, as are shown in the following section for Mg alloys, the lack of slip systems means very different material flow behaviour during FS and different deformation and fracture behaviours during tensile-shear testing

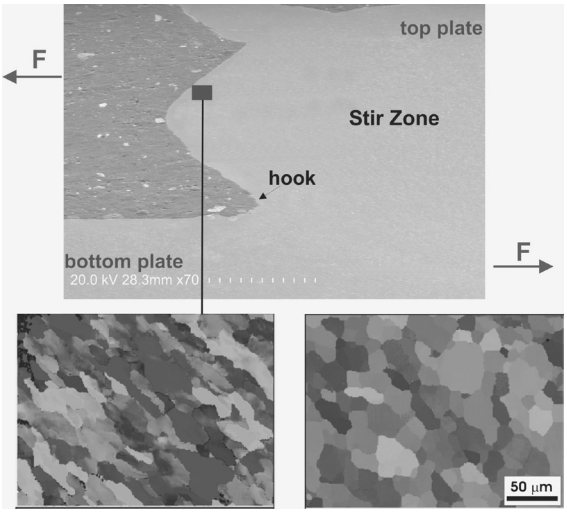

Fig. 13. Cross section of an A6060 tested sample (top) and EBSD orientation maps (bottom), bottom-left taken next to fracture surface and bottom-right away from the fracture surface in SZ

3.2. Mg alloy joint structure and strength

A high h hook of an AZ31B weld is shown in Fig. 14. The pin induced upward flow very effectively lifted the un-welded lap a long distance up. But, the sideward flow caused by the shoulder is very different to that during Al alloy FSLW and is very weak during this Mg alloy FSLW. This weak sideward flow has resulted in $\gamma << 0$.

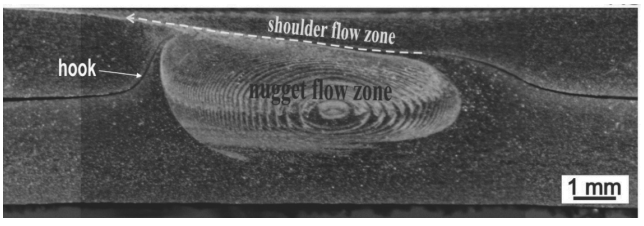

Fig. 14. Cross sectional view of an AZ31B weld made using ω = 1,000 rpm and v = 112 mm/min displaying a large hook

Details of the hook in Fig. 14 can be examined further using a higher magnification, shown in Fig. 15 (left). It is clear that the hook is fully continued to the very end of the hook, further suggesting that there was little sideward flow to affect the hook. Reducing ω value from 1,000 rpm to 500 rpm reduced the pin induced upward flow and thus reduced considerably the h value from 1.34 mm to 0.28 mm. There must not a sideward flow in that region and γ is close to 0.

The hook features shown in Figs. 14 and 15 can be compared to those in Fig. 8, for welds made using ω = 500 rpm or 1,000 rpm and v = 112 mm/min. Although the upward flows cannot be clearly compared, it can be concluded that the sideward flow (plastic deformation) was clearly very weak during FSLW of AZ31B. This is consistent with the lack of slip systems in this alloy.

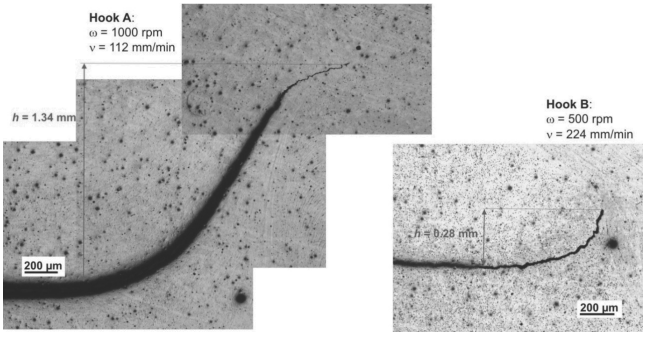

Fig. 15. Micrographs of two hooks of AZ31B welds, ω = 1,000 rpm (left) and = 500 rpm (right), v = 112 mm/min

Strength values plotted as a function of h are presented in Fig. 16. Strength values for butt FS welds are greater than 200 MPa [23] and for b = 2.5 mm we should expect the strength equivalent (F_m/w_s) > 500 N/mm. As shown in Fig. 16, when $h \rightarrow 0$, $F_m/w_s \approx 255$ N/mm and thus, F_m/w_s (lap) << F_m/w_s (butt). This is clearly different to Al alloy FSLW where when $h \rightarrow 0$ F_m/w_s (lap) ≈ F_m/w_s (butt). The F_m/w_s (butt) refers to the maximum value of strength equivalent for butt welds.

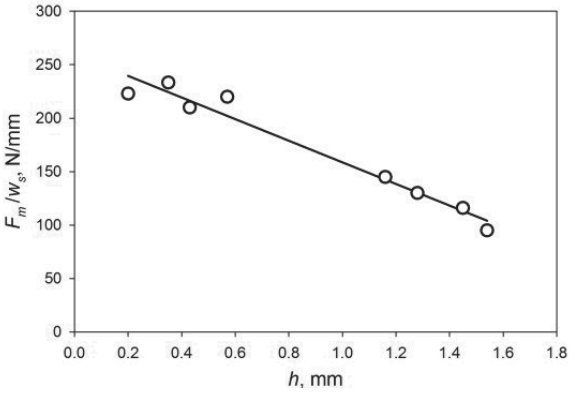

Fig. 16. Strength values plotted as a function of hook size for AZ31B welds

All Mg lap weld samples fractured in hook locations, as shown in Fig. 17 for two samples with very different hook sizes. Examining these tested samples also suggests little local bending and thus little deformation before the final fracture. This is very different from the high amount of local deformation in Al alloy samples, as already described. Little local deformation and bending mean that the high stress concentration cannot be relaxed. As suggested in Fig. 11, the effective stress in the hook region should be at least 3 times of the applied stress. This un-relaxed stress concentration is thus the reason why F_m/w_s (lap) << F_m/w_s (butt).

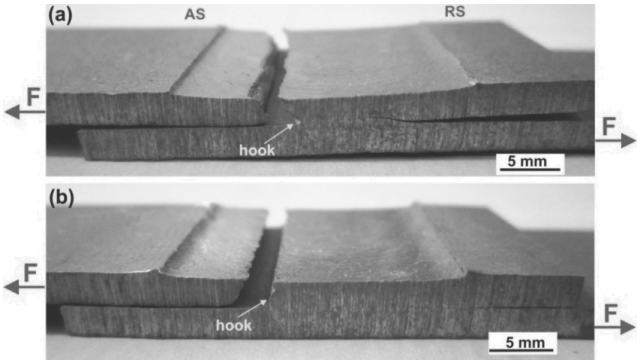

Fig. 17. Tensile-shear tested samples of AZ31B welds displaying fracture in hook location (top: h = 0.28 mm, and bottom: h = 1.34 mm)

Microstructures of a tested sample are shown in Fig. 18. The SZ featuring recrystallized grains as the result of the thermomechanical processing during FS is the same as that in the SZ of Al alloy FSL welds, as shown in Fig. 14. The features of deformation in the region adjacent to the fracture surface in AZ31B welds (Fig. 18) are completely different from that in A6060 welds. The grains are not seen elongated suggesting little plastic deformation by slip. Dense twins are observed, suggesting that in the highly stress concentrated region the material deformed by twinning but the total amount of deformation must be quite low before fracturing. These observations are in common with the known deformation behaviours of this alloy, particularly the feature of little necking during tensile testing.

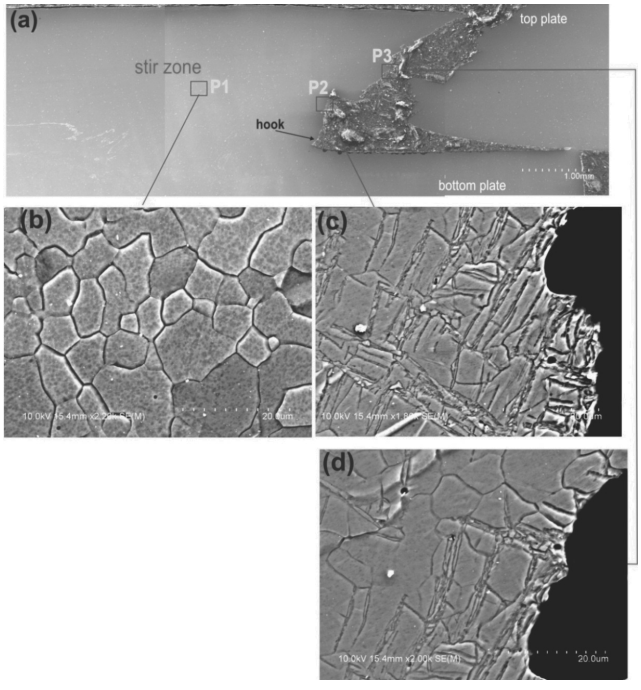

Fig. 18. Cross section of an AZ31B tested sample

3.3. Al-to-steel joint structure and strength

Only two selected samples are shown here to illustrate the importance of interface microstructures and based on this illustration a suggestion of FSLW control for maximum strength can then be made. Fig. 19 is the first example and a mixed stir zone (MSZ) commonly observed [20-22] is shown between the top Al plate and the bottom steel plate. The area of MSZ largely corresponds to the area of the pin penetrated into steel (in a 2D cross section) and this zone is a mixture of Fe-Al intermetallic thin pieces embedded in the recrystallized α-Fe grains.

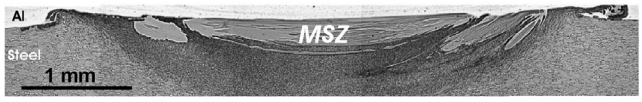

Fig. 19. Cross sectional view of an Al-to-steel weld made with ω = 1,400 rpm, v = 20 mm/min and $D_p \approx$ 0.3 mm displaying MSZ

With a MSZ, a metallurgical bond between Al and steel is established and thus a slight pin penetration (a slight positive D_p value, referring to Fig. 3) is commonly believed to be the condition for a good weld strength [20-22]. Naturally, a MSZ cannot form and if $D_p << 0$. However, FS tool can be position controlled so that $D_p \approx 0$. In this case, although there can still be an absence of MSZ, a thin Fe-Al interface intermetallic layer can form, metallurgically bonding the top and bottom plates together, as demonstrated by an example shown in Fig. 20.

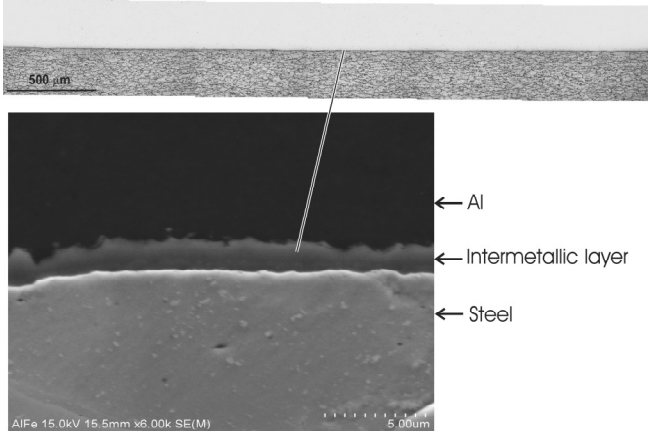

Fig. 20. Cross sectional view of an Al-to-steel weld made with ω = 1,400 rpm, v = 20 mm/min and $D_p \approx$ 0 mm displaying no MSZ but an interface layer

Two examples of tensile-tested curves are shown in Fig. 21 for the two different D_p conditions. For the penetrated sample, the amount of deformation before final fracture and thus fracture energy are not low. The weld strength at 299 N/mm is significantly higher than that of Mg FSL welds (255 N/mm) but is considerably lower than that of Al FSL welds (> 400 N/mm), for h = 0.

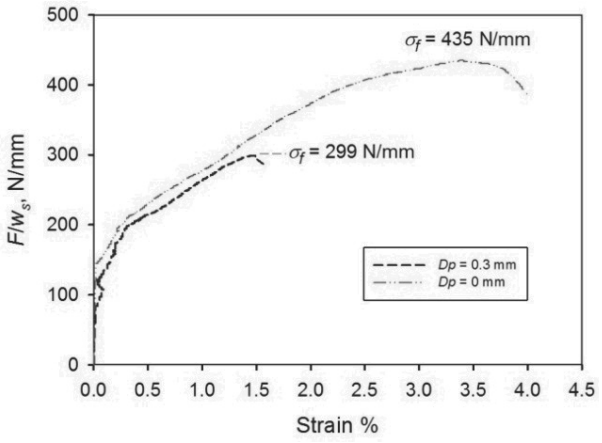

Fig. 21. Tensile-shear curves of two samples of welds made with ω = 1,400 rpm, v = 20 mm/min and D_p values as indicated

The weld strength at 299 N/mm is close to the values of ~ 315 N/mm which is the maximum value for a large group of samples using a slight pin penetration [22]. In this latter study, when a weld is free of macro-defects the strength equivalent value is close to that maximum value, regardless of what the FS speed condition was. In order to understand this, an analysis was conducted on a specially tested sample in the present work. As is clearly shown in Fig. 22, cracks propagated in MSZ, likely along the more brittle Fe-Al intermetallic pieces and occasionally stopped by the tougher α-Fe grains. If this is the common fracture feature and the required fracture strength will then be similar once a MSZ is established, regardless of what the FS condition is so long as the weld is free of macro-defects.

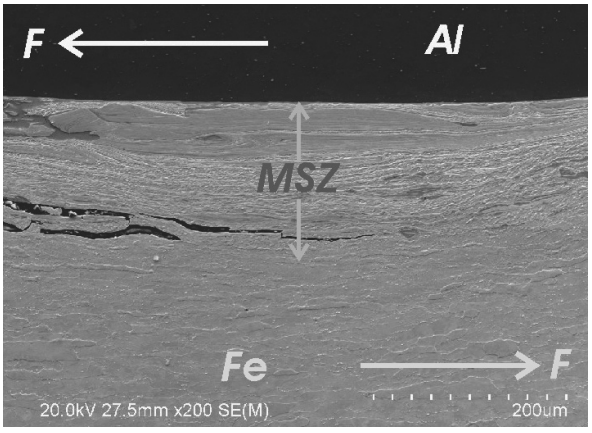

Fig. 22. SEM micrograph taken in MSZ region of a weld made with ω = 1,400 rpm, v = 20 mm/min and $D_p \approx$ 0.3 mm and tested to 270 N/mm (~ 90 F_m/w_s)

When $D_p \approx 0$ and an interface layer is established without MSZ, as shown in Fig. 21, fracture strength (435 N/mm) is considerably higher than that for the sample with MSZ (299 N/mm). The amounts of deformation and fracture energy as indicated by the curve suggest a considerably tougher weld made by the zero D_p condition. These are clear by viewing the tested samples in Fig. 23. For the pin penetrated sample ($D_p \approx$ 0.3 mm), the sample having been slightly bent is evident. On the other hand, for the zero D_p sample, a large amount of local deformation and bending before the final fracture is clearly the feature. The absence of MSZ in the zero D_p sample means a different fracture behaviour. The large amounts of deformation and fracture energy for this sample means that the thin interface layer is not brittle under tensile-shear condition. From the present results, it can be suggested that careful positioning control for Al-to-steel FSL welds is a mean for the optimal weld strength to be obtained.

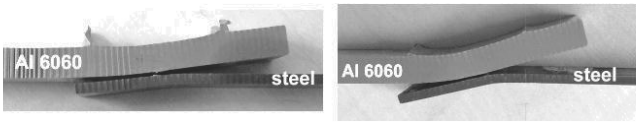

Fig. 23. Tensile-shear tested samples of welds made with ω = 1,400 rpm, v = 20 mm/min and (a) $D_p \approx$ 0.3 mm and (b) $D_p \approx$ 0 mm

4. Conclusions

The size (h), orientation (γ) and continuity of a hook formed during friction stir lap welding (FSLW) of Al-to-Al, using A6060, are FS material flow dependent. While the pin related flow is fundamental for hooking to form, γ and continuity are determined by shoulder related flow. For $h \rightarrow 0$, strength of a weld by tensile-shear testing (F_m/w_s) is largely the same as the strength of a bead-on-plate sample. In both cases, FS softening dominates and stress concentration (σ_c) does not affect F_m/w_s significantly due to local bending to reduce considerably σ_c. Thinning effect on F_m/w_s due to hooking can be marked by the effect of softening when h is not very high. During FSLW of Mg-to-Mg, using AZ31B, shoulder related flow is very weak which results in little reduction in h, little hook reorientation and little reduction in hook continuity. For Mg-to-Mg welds, F_m/w_s (lap) << F_m/w_s (butt), due to σ_c effect. The deformation behaviours during FS and tensile-shear testing are consistent with the limited slip systems in Mg. Finally, for FSLW of Al-to-steel, pin penetration to form mixed stir zone (MSZ) is a condition for a reasonable strength. Position control for forming a continued interface layer only without forming MSZ results in a considerably higher F_m/w_s value.

References

[1] W.M. Thomas, J.C. Needham, M.G. Murch, P. Templesmith, C.J. Dawes, G B Patent Application No. 9125978.8, 1991.
[2] S.W. Kallee, D. Lohwasser, Chen Z. (Ed), Friction Stir Welding - from basics to application, Woodhead Publishing, Cambridge, 2010.
[3] R.S. Mishra, Z.Y. Ma, Friction stir welding and processing, Materials Science and Engineering R 50 (2005) 1-78.
[4] R. Nandana, T. DebRoya, H.K.D.H. Bhadeshia, Recent advances in friction-stir welding - Process, weldment

tructure and properties, Progress in Materials Science 53 (2008) 980-1023.
[5] P.L. Threadgill, A.J. Leonard, H.R. Shercliff, P.J. Withers, Friction stir welding of aluminium alloys, International Materials Review 54 (2009) 49-93.
[6] L.E. Murr, Structure, synthesis, and chemical reactions of fluorinated cyclopropanes and cyclopropenes, Journal of Materials Engineering and Performance 19 (2010) 1071-1098.
[7] R. Rai, A. De, H.K.D.H. Bhadeshia, T. DebRoy, Review: friction stir welding tools, Science and Technology of Welding and Joining 16 (2011) 325-342.
[8] G. Cam, Friction stir welded structural materials: beyond Al-alloys, International Materials Reviews 56 (2011) 1-48.
[9] Y.N. Zhang, X. Cao, S. Larose, P. Wanjara, Review of tools for friction stir welding and processing, Canadian Metallurgical Quarterly 51 (2012) 250-261.
[10] L. Cederqvist, A.P. Reynolds, Factors affecting the properties of friction stir welded aluminum lap joints, Welding Journal - Research Supplementary 80 (2001) 281-287.
[11] M. Ericsson, L. Jin, R. Sandström, Fatigue properties of friction stir overlap welds, International Journal of Fatigue 29 (2007) 57-68.
[12] D. Fersini, A. Pirondi, Fatigue behaviour of Al2024-T3 friction stir welded lap joints, Engineering Fracture Mechanics 74 (2007) 468-480.
[13] G. Buffa, G. Campanile, L. Fratini, A. Prisco, Friction stir welding of lap joints: Influence of process parameters on the metallurgical and mechanical properties, Materials Science and Engineering A 519 (2009) 19-26.
[14] M.K. Yadava, R.S. Mishra, Y.L. Chen, B. Carlson, G.J. Grant, Study of friction stir joining of thin aluminium sheets in lap joint configuration, Science and Technology of Welding and Joining 15 (2010) 70-75.
[15] L. Dubourg, A. Merati, M. Jahazi, Process optimization and mechanical properties of Friction Stir Lap Welds of 7075-T6 stringers on 2024-T3 skin, Materials and Design 31 (2010) 3324-3330.
[16] X. Cao, M. Jahazi, Effect of tool rotational speed and probe length on lap joint quality of a friction stir welded magnesium alloy, Materials and Design 32 (2011) 1-11.
[17] S. Yazdanian, Z.W. Chen, G. Littlefair, Effects of friction stir lap welding parameters on weld features on advancing side and fracture strength of A6060-T5 welds, Journal of Materials Science 47 (2012) 1251-1261.
[18] E. Taban, J.E. Gould, J.C. Lippold, Dissimilar friction welding of 6061-T6 aluminum and AISI 1018 steel: Properties and microstructural characterization, Materials and Design 31 (2010) 2305-2311.
[19] G. Liedl, R. Bielak, J. Ivanova, N. Enzinger, G. Figner, J. Bruckner, M. Pasic, M. Pudar, S. Hampel, Joining of aluminum and steel in car body manufacturing, Physics Procedia 12 (2011) 150-156.
[20] A. Elrefaey, M. Gouda, M. Takahashi, K. Ikeuchi, Characterization of aluminum/steel lap joint by friction stir welding, Journal of Materials Engineering and Performance 14 (2005) 10-17.
[21] K. Kimpapong, T. Watanabe, Lap joint of A5083 aluminum alloy and SS400 steel by Friction Stir Welding, Materials Transactions 46 (2005) 835-841.
[22] M. Movahedi, A.H. Kokabi, S.M. Seyed Reihani, H. Najafi, Mechanical and microstructural characterization of Al-5083/St-12 lap joints made by friction stir welding, Procedia Engineering 10 (2011) 3297-3303.
[23] S.M. Chowdhury, D.L. Chen, S.D. Bhole, X. Cao, Tensile properties of a friction stir welded magnesium alloy: effect of pin tool thread orientation and weld pitch, Materials Science and Engineering A 527 (2010) 6064-6075.